J Mater Sci (2010) 45:4866–4870
DOI 10.1007/s10853-010-4587-0

ULTRAFINE GRAINED MATERIALS

Spheroidization of medium carbon steel fabricated by continuous shear drawing

Young Gun Ko · Seung Namgung · Dong Hyuk Shin · Il Heon Son · Ki Ho Rhee · Duk-Lak Lee

Received: 10 February 2010 / Accepted: 30 April 2010 / Published online: 14 May 2010

Abstract This study was undertaken to propose a method of continuous shear drawing (CSD) for industrial applications to steel-wire manufacturing. The study compared the spheroidization behavior of medium carbon steel processed by CSD to that processed via conventional drawing. Microstructural observation revealed that the use of the CSD method was effective for deforming the pearlite colonies, resulting in wavy pearlitic cementites without noticeable cracks on the surface. After annealing treatment at a subcritical temperature of 973 K for 1 h, the CSD-deformed sample exhibited a uniform microstructure with a number of fine globular cementites that was greater in extent than that by drawing; this result was mainly due to the easy spheroidization triggered by the CSD strain.

Introduction

Over the last decade, severe plastic deformation of metals and alloys utilizing equal channel angular (ECA) pressing has been regarded as a promising method to tailor the ultrafine-grained microstructure, which might exhibit better mechanical performance as compared to the coarse and fine-grained counterparts [1–4]. In addition to grain refinement, the ECA pressing technique has been found to be beneficial for fragmenting the rigid lamellar structure of ferrous alloys through the decomposition of pearlitic cementite to promote plasticity during further deformation. Thus, this method would be put to use for commercial applications in steel-wire manufacturing if an obstacle arising from ECA pressing itself, in which the deformation and processing of workpieces were not continuous, would be solved. One of the moves to develop a method suitable for continuous processing was the use of ECA drawing, in which samples are deformed in a drawing manner instead of a pressing one, because the length of the workpiece was likely no longer to be limited by the buckling instability of both the sample and the plunger during deformation due to compressive loading [5–8]. However, Luis et al. [7] have reported using finite element method (FEM) calculation validated with actual experiments that show, in terms of keeping the original segment of samples, deformation of ECA drawing fairly differed from that of ECA pressing, giving rise to the occurrence of an appreciable corner gap to be formed between sample and die, as shown in Fig. 1a. The deformation of samples seemed more dominated by drawing than by shearing when samples went through the shear zone where two channels met. Extensive necking and inferior mechanical properties would be expected. Although comprehensive understanding of the relationship between two die-angles and strain has been well established [9], it is still of interest to know how, particularly in the case of ECA drawing, the angle of the die and the diameter of the exit channel influenced deformation.

It is our main purpose to suggest a new type ECA drawing, termed continuous shear drawing (CSD), with an effort to modify the design of the die to reduce the dimensional inhomogeneity of the sample. Once the optimum condition for uniform shear deformation of medium

Y. G. Ko
School of Materials Science and Engineering,
Yeungnam University, Gyeongsan 712-749, Korea

S. Namgung · D. H. Shin (✉)
Department of Metallurgy and Materials Science,
Hanyang University, Ansan 426-791, Korea
e-mail: dhshin@hanyang.ac.kr

I. H. Son · K. H. Rhee · D.-L. Lee
Wire Rod Research Group, Technical Research Laboratory,
POSCO, Pohang 790-785, Korea

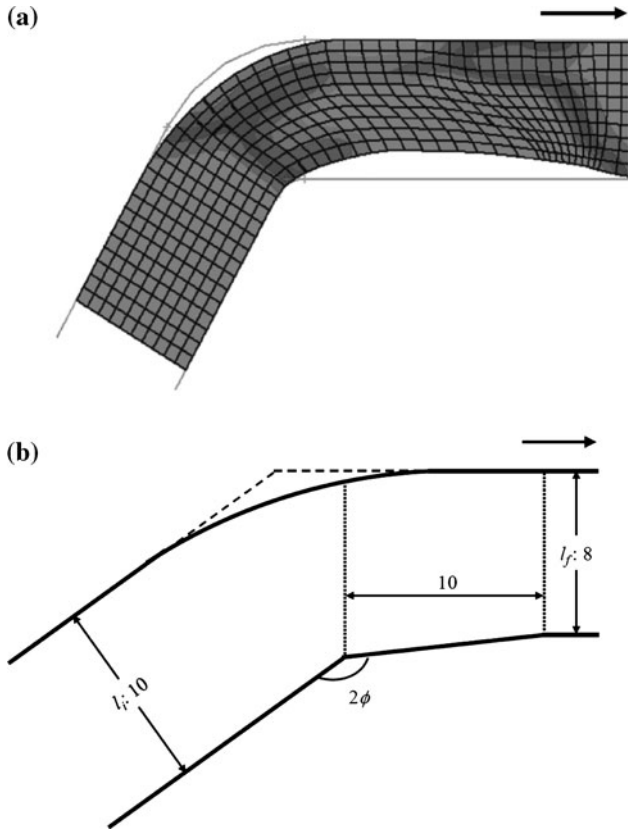

Fig. 1 **a** FEM result showing the deformation behavior of sample during ECA drawing with a die having specific inner angle of 120° [6] and **b** the schematic diagram of the present die used for CSD deformation ($2\phi \sim 135°$)

carbon steel is determined, the effect of the CSD strain on spheroidization during subsequent annealing was studied and compared to that of conventional drawing strain.

Experimental procedures

A plastic deformation was imposed on medium carbon steel wire (diameter: 10 mm) with a chemical composition of Fe-0.36C–0.25Si–0.73Mn–0.33P–0.33S in wt%, by means of the CSD technique with a drawing speed of 100 mm/min, corresponding to a strain rate of 0.3/s (Fig. 1b) [10]. To compare the deformation and spheroidization behavior during annealing, conventional drawing on a die with a diameter of the entrance channel of 10 mm and of the exit channel of 8 mm was also carried out. The initial microstructure of the medium carbon steel consisted of approximately 90% pearlite phase; the remainder was of ferrite phase. In the pearlite colonies, both the lamellar spacing and the cementite thickness were measured to be ~0.4 μm. There were some kinks and breaks in the carbide plates. To evaluate the spheroidization of the deformed pearlitic cementite, annealing treatment at a subcritical temperature of 973 K for 1 h followed by furnace cooling was performed. A_1 temperature of this steel was determined based on the available equation reported by Rocha et al. [11]. The microstructural examination through scanning-electron microscopy (SEM, JEM-6330F) was conducted on the deformed samples etched with 3% nital solution.

Continuous shear drawing

According to earlier work on the deformability of workpieces during ECA drawing, upper bound analysis [6] and FEM perspective [7] predicted that the use of ECA drawing obviously resulted in unstable deformation of individual meshes when the inner angles became less than 120°. As shown in Fig. 1a, the corners of the die were not completely filled by the samples. Thus, non-uniform deformation was evident since the sample was more bent rather than sheared. In this study, a die having an inner angle of 135° was designed to avoid the formation of pronounced necking, which is noxious to further deformation and mechanical properties. Besides, the CSD die was prepared by reducing the diameter of the exit channel to impose much higher strain, as compared to the process in ECA drawing. Considering the reduced exit channel diameter, an additional strain was imparted when the samples experienced CSD deformation. The total stain (ε_T) accumulated from the present CSD can be seen as the sum of the shear strain [12] and the drawing strain, as follows,

$$\varepsilon_T = \left(2/\sqrt{3}\right) \cdot \cot\phi + \ln(l_i/l_f) \quad (1)$$

in which ϕ, l_i, and l_f are the half of inner angle in the die, the initial, and the final diameters of the sample, respectively. A detailed description of the tooling, together with an effective strain, is listed in Table 1. Among the variables affecting both total strain and deformation, the role of the outer angle should be considered. However, that role was not taken into account in this study since the effect of the outer angle is not significant when the sample is deformed in a die with an inner angle of more than 120° [13].

Results and discussion

Figure 2 displays a macroscopic view of medium carbon steels after deformation. Figure 2a is related to the sample deformed by conventional drawing, while Fig. 2b is associated with the sample deformed via CSD operation. Deformation speed and temperature are the same. The direction of deformation was from left to right. Both deformed samples exhibited good surface quality without

Table 1 Description of two dies and estimated strain

Die	Inner angle (°)	Shear strain	Diameter (mm)		Drawing strain	Total strain
			Entrance	Exit		
Drawing	–	–	10	8	0.22	0.22
CSD	135	0.48	10	8	0.22	0.70

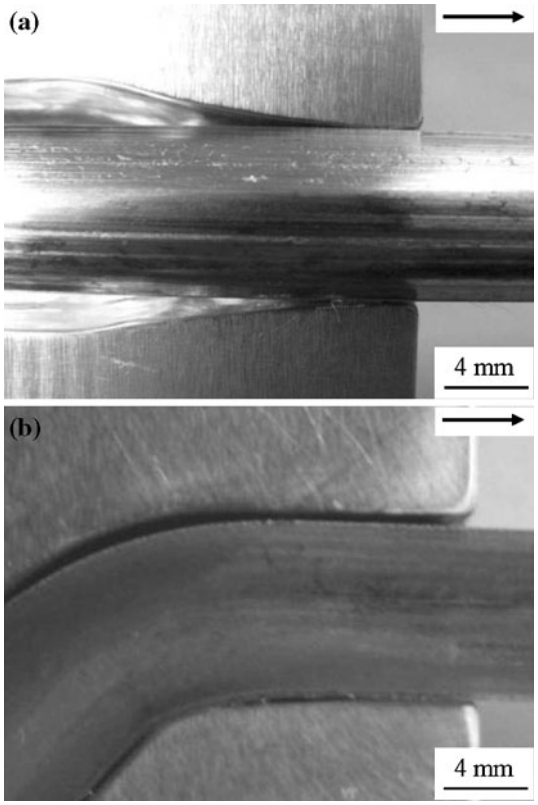

Fig. 2 Macrographs of medium carbon steel wires after **a** drawing and **b** CSD deformation

surface cracks and were clearly flattened toward the deformation direction as well. This fact indicated that the CSD die was sufficient to constrain the sample and imparted fairly uniform strain to the sample. Figure 3 displays the load–stoke curves during CSD deformation. The loads of samples were apt to rapidly increase and reached a steady state, but higher values of load were observed during CSD than during drawing. As shown in Table 1, the total strain by CSD was three times higher than that by drawing. Thus, high load was due to strain hardening of sample by high strain.

Figure 4 shows microscopic images revealing the microstructure change of pearlitic cementite phases in medium carbon steels following drawing and CSD deformation. Regardless of deformation methods used, it is obvious that no pearlite colonies remained unchanged, but the apparent morphologies differ considerably due to varied strain and deformation modes.

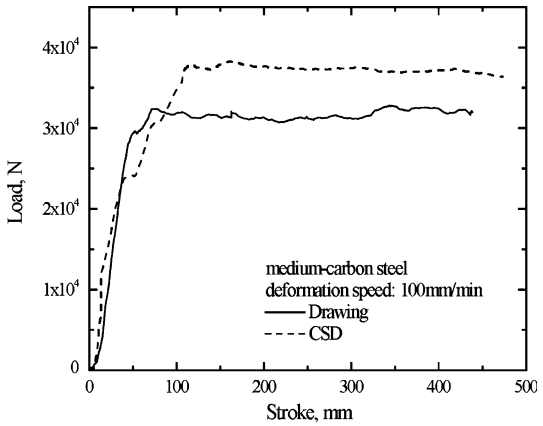

Fig. 3 Measured load–stroke curves for medium carbon steel wires

After the drawing processing, most of the pearlite were deformed, inclined persistently to the drawing direction (Fig. 4a) while some cementites were curled [14, 15]. According to earlier reports on the deformation of pearlitic steels whose colonies were randomly oriented prior to severe cold drawing [16, 17], paralleled cementite plates were clearly found on the planes of the lamellae that were aligned along the drawing axis. On the other hand, curled/kinked cementites were observed on the planes of the lamellae that are not aligned along the drawing axis since they could accommodate the external strain through bending instead of moving whole colonies to the drawing direction. Thus, the changes of the cementite morphologies were largely affected by the orientation difference between the loading axis and the pre-existing directions of the pearlite colonies. As to the microstructure deformed via CSD method (Fig. 4b), depending on various inclinations of the pearlite structure with respect to the shear direction determined by the inner angle, some cementite were present in the form of curled and wavy structures, while others kept their original lamellar structure; however, necked cementites were still detected. In general, there existed two distinct modes that were used to describe the deformation of duplex alloys as per the rule of mixture relationships, such as iso-stress and iso-strain modes. Since most ferrite grains, working as a soft phase within the pearlite colonies, deformed much easier than cementite, deformation was thought to obey iso-stress mode rather than iso-strain mode, implying that the plasticity was mainly controlled by the ferrite phases. In an iso-stress

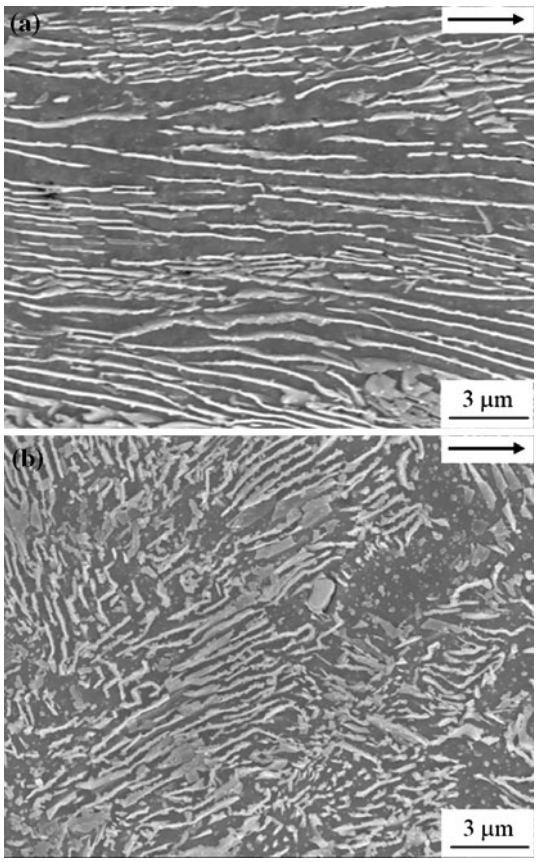

Fig. 4 SEM images showing deformed microstructures after **a** drawing and **b** CSD deformation. *White* and *dark* regions are cementite and ferrite. *Arrow* indicates the flow direction

mode in which the stresses were equally distributed to deformation of the hard and the soft phases, the amount of strain was in part accommodated by the hard cementite phases, as can be seen in Fig. 4b. This result was consistent with the earlier TEM observations showing the significant morphological changes in cementite phases despite the poor ductility of cementite, which has a monoclinic crystal structure [18]. This was of great importance since a number of the carbon atoms at the tip of the kinked (or breakup) cementite phases were diffused with ease to low-energy sites such as the flat platelet surface [19–21]. As a result, the wavy pearlite and fragmented cementite played a key role in accelerating the evolution of spheroidization during subsequent heat treatment.

For the annealing behavior of the samples at a subcritical temperature of 973 K with no prior deformation, conventional drawing and CSD processes are shown in Fig. 5. Particles with an aspect ratio of less than two were considered to be fully spheroidized. Figure 5a is the annealed microstructure of the initial sample that experienced no deformation prior to the subcritical annealing treatment, revealing that thin-striped cementite phases still existed as remnants. This fact indicated that subcritical

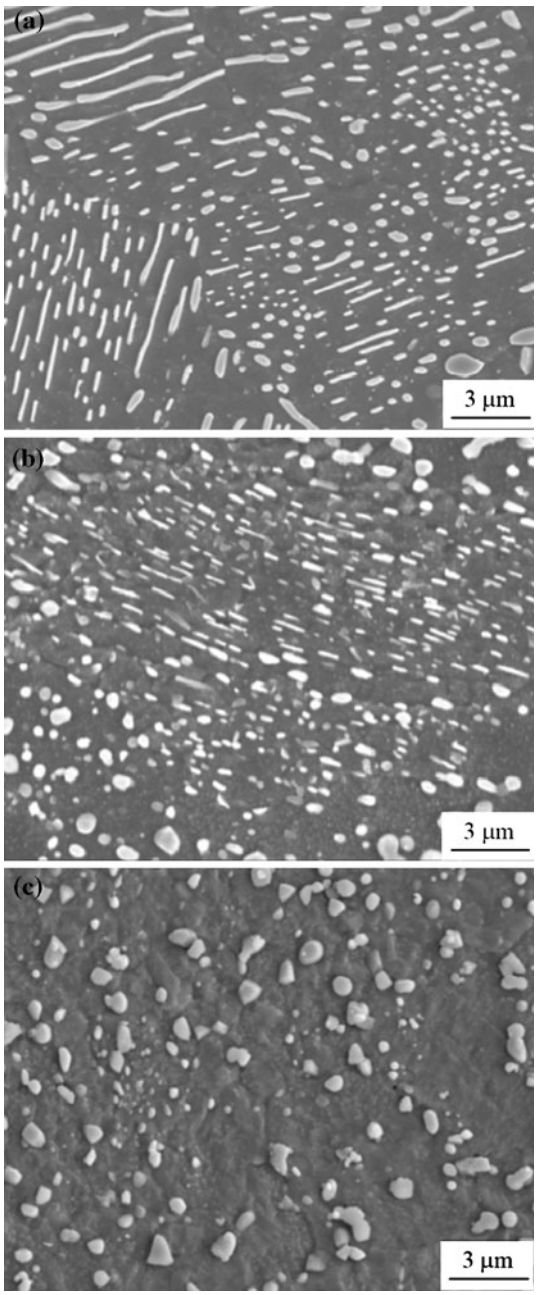

Fig. 5 SEM images showing spheroidization behavior at a subcritical temperature of 973 K **a** for 10 h in sample with no prior deformation, **b** for 5 h in sample deformed via conventional drawing, and **c** for 1 h in sample deformed via CSD method

annealing for 10 h was insufficient to attain a homogeneous microstructure containing fine globular carbide particles. On the other hand, the samples deformed through drawing and CSD methods needed 5 and 1 h, respectively, to attain a homogeneous microstructure, as shown in Fig. 5b and c. It is found that, when the CSD method ($\varepsilon \sim 0.70$) was used, the rate of spheroidization was much faster than that when the sample was deformed via conventional drawing ($\varepsilon \sim 0.22$). It is worth mentioning that

the driving force for spheroidization was the reduction in area of the ferrite–cementite interface by the conversion of carbide plates to spheroids. And, such rate for spheroidization was triggered with an increment in the plastic strain prior to annealing treatment. Accordingly, by inducing the high level of strain to materials in shear causing large stored energy, the use of CSD method seemed more beneficial for reducing total time required for spheroidization. The same issues could be found in the deformation of ultra-high carbon steel based on a divorced eutectoid transformation-associated deformation [22]. Zhang et al. [21] demonstrated that a resultant microstructure with spheroidal cementite of $\sim$0.6 μm in size dispersed on the ferrite matrix was obtained when the sample was deformed at a temperature of 973 K and reduction of 60% under compressive loading. Indeed, Sun et al. [23] reported on a deformed microstructure consisting of equiaxed ferrite grains and nearly spheroidized cementite particles by means of warm cross-wedge rolling at 953 K. However, such forming methods were carried out in a high-temperature region. From a standpoint of stored energy as a chemical driving force for microstructural changes, it is more desirable for steel-wire to be deformed at room temperature than at temperatures above 950 K unless sample failure during deformation is observed to occur. Hence, we believe that the CSD process suitable for deformation at room temperature was successfully established in this study, which makes it possible to drive down the cost.

From the results obtained, the proposed CSD method may have industrial potential in the process of steel-wire manufacturing, and can be applied as an intermediate step prior to a batch annealing treatment, allowing us to reduce annealing time significantly by promoting a fast rate of spheroidization of the pearlitic cementite phase. In earlier investigations [20, 24, 25], however, it was found necessary to require intense strain of higher than $\sim$4 to refine the ferrite phase grains down to a micrometer level, as well as to attain the fine arrays of spheroidized cementite solely during deformation. A detailed study of the deformation and microstructure change with an increasing amount of CSD strain will be required to provide better understanding of the practical applications of the CSD technique.

Conclusion

A CSD method was employed to explore the possibility of fabricating a wire product of medium carbon steel. Using a well-prepared die with an inner angle of 135° and an exit diameter 8 mm, sound deformation of medium-carbon steel took place. When compared to the results of conventional drawing, the use of the CSD technique accompanied by subcritical annealing treatment led to a resultant microstructure with fine equiaxed cementites dispersed uniformly on the ferrite matrix due to easy spheroidization triggered by CSD strain.

References

1. Furukawa M, Horita Z, Nemoto M, Langdon TG (2001) J Mater Sci 36:2835. doi:10.1023/A:1017932417043
2. Yoon SC, Kim HS (2009) J Kor Inst Met Mater 47:699
3. Valiev RZ, Estrin Y, Horita Z, Langdon TG, Zehetbauer MJ, Zhu YT (2006) JOM 58:33
4. Kim YG, Ko YG, Shin DH, Lee S (2009) J Kor Inst Met Mater 47:397
5. Chakkingal U, Suriadi AB, Thomson PF (1999) Mater Sci Eng A 266:241
6. Alkorta J, Rombouts M, Messenmaeker JD, Froyen L, Sevillano JG (2002) Scripta Mater 47:13
7. Luis CJ, Garcés Y, González P, Berlanga C (2002) Mater Manuf Proc 17:223
8. Zisman AA, Rybin VV, Van Boxel S, Seefeldt M, Verlinden B (2006) Mater Sci Eng A 427:123
9. Saito Y, Utsunomiya H, Suzuki H, Sakai T (2000) Scripta Mater 42:1139
10. Ko YG, Shin DH, Lee CS (2009) J Mater Res 24:2161
11. Rocha RO, Melo TMF, Perelom EV, Santos DB (2005) Mater Sci Eng A 391:296
12. Segal SL (1995) Mater Sci Eng A 197:157
13. Nakashima K, Horita Z, Nemoto M, Langdon TG (1998) Acta Mater 46:1589
14. Song YS, Kim DW, Yang HS, Han SH, Chin KG, Choi SH (2009) J Kor Inst Met Mater 47:274
15. Yang YS, Bae JG, Park CG (2008) J Kor Inst Met Mater 46:111
16. Bae CM, Nam WJ, Lee CS (1996) Scripta Metall 35:641
17. Park DB, Lee JW, Lee YS, Park KT, Nam WJ (2009) Metal Mater Int 15:197
18. Inoue A, Ogura T, Masumoto T (1977) Trans JIM 17:1201
19. Tian YL, Kraft RW (1987) Metall Trans A 18:1403
20. Hono K, Ohnuma M, Murayama M, Nishida S, Yoshie A, Takahashi T (2001) Scripta Mater 44:977
21. Zhang SL, Sun XJ, Dong H (2006) Mater Sci Eng A 432:324
22. Oyama T, Sherby OD, Wadsworth J, Walser B (1984) Scripta Metall 18:799
23. Sun SH, Xiong Y, Zhao J, Lv ZQ, Li Y, Zhao DL, Fu WT (2005) Scripta Mater 53:137
24. Shin DH, Kim BC, Kim YS, Park KT (2000) Acta Mater 48:2247
25. Okitsu Y, Takata N, Tsuji N (2008) J Mater Sci 43:7391. doi:10.1007/s10853-008-2971-9